



HAL
open science

Size patterns of the coccolith *Watznaueria barnesiae* in the lower Cretaceous: Biotic versus abiotic forcing

Barbara Gollain, Emanuela Mattioli, Samer Kenjo, Annachiara Bartolini, Stéphane Reboulet

► To cite this version:

Barbara Gollain, Emanuela Mattioli, Samer Kenjo, Annachiara Bartolini, Stéphane Reboulet. Size patterns of the coccolith *Watznaueria barnesiae* in the lower Cretaceous: Biotic versus abiotic forcing. *Marine Micropaleontology*, 2019, 152, pp.101740. 10.1016/j.marmicro.2019.03.012 . hal-02293290

HAL Id: hal-02293290

<https://univ-lyon1.hal.science/hal-02293290>

Submitted on 21 Jul 2022

HAL is a multi-disciplinary open access archive for the deposit and dissemination of scientific research documents, whether they are published or not. The documents may come from teaching and research institutions in France or abroad, or from public or private research centers.

L'archive ouverte pluridisciplinaire **HAL**, est destinée au dépôt et à la diffusion de documents scientifiques de niveau recherche, publiés ou non, émanant des établissements d'enseignement et de recherche français ou étrangers, des laboratoires publics ou privés.



Distributed under a Creative Commons Attribution - NonCommercial 4.0 International License

1 Size patterns of the coccolith *Watznaueria barnesiae* in the lower Cretaceous: biotic *versus*
2 abiotic forcing

3

4 Barbara Gollain¹, Emanuela Mattioli^{2,3*}, Samer Kenjo^{2,4}, Annachiara Bartolini⁵, Stéphane
5 Reboulet²

6

7 ¹ Jardin des Sciences, Université de Strasbourg, 12 rue de l'Université, F-67000 Strasbourg,
8 France.

9 ² Université de Lyon, UCBL, ENSL, CNRS, LGL-TPE, F-69622 Villeurbanne, France.

10 ³ Institut Universitaire de France, Paris, France.

11 ⁴ Department of Geology, Faculty of Sciences, Damascus University, Syria

12 ⁵ Muséum National d'Histoire Naturelle Paris, UMR 7207 CNRS - CR2P, France

13

14 * corresponding author: emanuela.mattioli@univ-lyon1.fr

15

16 **Abstract**

17

18 Bodysize is a major trait allowing the assessment of the respective control of evolution *vs.*
19 (palaeo)environment on unicellular micro-organisms. Size patterns can be retraced for
20 fossilisable micro-organisms, especially for coccolithophores, over geological time spans.
21 Here, we present coccolith size patterns of *Watznaueria barnesiae*, which was a dominant and
22 ubiquitous taxon in the Mesozoic. Measurements were conducted at two sites spanning the
23 Upper Berriasian to Lower Hauterivian, namely the Vergol-La Charce section in the
24 epicontinental Vocontian Basin, and the ODP site Leg 185 Hole 1149B located in the
25 Nadezhda Basin, in the Pacific Ocean. The obtained results were treated using multivariate
26 analysis in order to detect significant trends of the measured parameters. Size values of
27 coccoliths from both sites are remarkably similar and display comparable patterns, namely a
28 statistically significant increase in the Lower Valanginian until maximum sizes recorded in
29 the aftermath of the Weissert event (Upper Valanginian). Although *W. barnesiae* coccolith-
30 size fluctuations, in the short term, might be related to environmental changes, the observed
31 long-term size patterns are interpreted as the result of directional selection, in which a single
32 phenotype is favoured through time. Comparison with data available in the literature shows a
33 return to a smaller size after the Turonian.

34 **Keywords:** Coccolith; biometry; *Watznaueria barnesiae*; Lower Cretaceous;
35 palaeoenvironment; evolution.

36

37 **1. Introduction**

38

39 In modern oceans, the size patterns of marine phytoplankton communities greatly affect food-
40 web structure and organic/inorganic carbon export into the ocean interior (Popp et al., 1998;
41 Hopkins et al., 2015). Body size is a major trait of organism's evolution. Of particular
42 relevance for unicellular organisms, is the fact that diffusion across the cell membrane,
43 especially passive diffusion, is strongly dependent on the surface-area/volume ratio (Lewis,
44 1976; Aloisi, 2015). Surface-area is proportional to length squared whilst volume is
45 proportional to length cubed, so unless cell-shape changes, larger cells need more resources
46 and produce more waste products, whilst diffusion becomes less efficient. The metabolic rates
47 of unicellular organisms are thus a function of this surface-area/volume ratio (e.g., Atkinson
48 et al., 2003; Fu et al., 2008; Key et al., 2010). In some coccolithophores, such as *Emiliana*
49 *huxleyi*, culture studies have shown a clear relationship between some physiological
50 parameters and the cell volume (Finkel et al., 2009).

51 Culture studies under controlled conditions or surface-water sampling in selected oceanic
52 settings allow us to observe the short-term responses of coccolithophore size to change in
53 physical or chemical parameters, such as the pH or the saturation state of ocean waters (e.g.,
54 Riebesell et al., 2000; Iglesias-Rodriguez et al., 2008; Beaufort et al., 2011). However, these
55 studies provide data that are limited in terms of time-duration, and do not allow testing of the
56 impact of evolution on organism's size changes.

57 With coccolithophores we have the chance to measure body size back in deep geological
58 time, to address questions about the relative importance of biotic controls (such as
59 competition, predation, grazing, infection, etc.) *versus* abiotic forcing (such as climate,
60 geography, extreme events, etc.) in shaping the evolution of life on Earth. One complication is
61 that coccolithophore fossils are predominately isolated coccoliths rather than complete
62 coccospheres. However, Henderiks (2008) has shown that for the dominant Cenozoic
63 placolith genera there is a linear relationship between coccolith and coccosphere sizes, and
64 that coccosphere size is proportional to cell size.

65 Here we present data on coccolith size changes of the species *Watznaueria barnesiae*, which
66 is the dominant coccolith in Lower Cretaceous sediments. This morpho-species is known for
67 its ubiquity in Mesozoic oceans (Mutterlose et al., 2005), and for its longevity (first

68 occurrence at the end of lower Toarcian for *W. fossacincta*, ~181 Ma, or Middle Jurassic,
69 ~168 Ma for *W. barnesiae*; last occurrence at ~64 Ma; Mattioli and Erba, 1999; Lees et al.,
70 2005). Biometry can be safely applied to *Watznaueria barnesiae* because this coccolith is
71 known for its resistance to diagenetic alteration (Roth and Krumbach, 1986). We have
72 predominantly measured isolated coccoliths, but whenever possible we also measured entire
73 coccospheres in order to test if the size relationships observed by Henderiks (2008) apply to
74 *Watznaueria*.

75 For this study, we selected Lower Cretaceous samples (upper Berriasian to basal Hauterivian;
76 ~140-133 Ma) from the Vocontian Basin, SE France (Vergol and La Charce composite
77 section; Fig. 1b). This section has been thoroughly studied for sedimentology (Greselle et al.,
78 2011), ammonite content (Reboulet, 1996; Reboulet and Atrops, 1999; Reboulet et al., 2003;
79 Reboulet and Rard, 2008; Kenjo, 2014; their ammonite zonal schemes are here updated
80 according to the standard zonation established by Reboulet et al., 2014; 2018), nannofossil
81 assemblages and geochemistry (Mattioli et al., 2014), and for biometric studies of
82 nannoconids (Barbarin et al., 2012). In order to discriminate the local *versus* global control on
83 coccolith size, we have used for comparison to the epicontinental Vocontian Basin samples
84 from the ODP Leg 185 Hole 1149B located in the Nadezhda Basin, in the Pacific Ocean (Fig.
85 1c; Plank et al., 2000). The two sites can be precisely correlated by nannofossil
86 biostratigraphy (Lozar and Tremolada, 2003; Mattioli et al., 2014). The Berriasian-
87 Hauterivian interval has been selected because it is characterised by a marked perturbation of
88 the carbon cycle indicated by a ~2‰ positive excursion of $\delta^{13}\text{C}_{\text{carb}}$, namely the Valanginian
89 Weissert event (Erba et al., 2004). This interval is also characterised by a nannoconid decline
90 (Erba and Tremolada, 2004), and is interpreted as a cool interlude within a global greenhouse
91 climatic period (Lini et al., 1992; Gréselle et al., 2011; Föllmi, 2012). This episode of well-
92 documented environmental change is thus ideal to determine whether such environmental
93 change impacted the morphology of *Watznaueria barnesiae* coccoliths.

94

95 Figure 1 approx. here

96

97 **2. Material and methods**

98

99 In this paper, specimens of *W. barnesiae* were measured along with *W. fossacincta*. This latter
100 form, which is rare in the studied samples, presents the same morphology as *W. barnesiae*,
101 but has a slightly open central area. *Watznaueria fossacincta* first occurred at the end of the

102 lower Toarcian (Mattioli and Erba, 1999), while *W. barnesiae*, which has a closed central
103 area, first occurred in the basal Bathonian (Mattioli and Erba, 1999; Fig. 2). Bornemann and
104 Mutterlose (2006) performed a biometric study on Albian *Watznaueria* and concluded that
105 there is no difference between these two morphotypes other than the central opening size,
106 which is a gradational character. They explicitly reject using them as two separate species.
107 Our observations suggest that this conclusion is valid for the entire Cretaceous. In the rest of
108 the text, we will refer to them as a single entity, *W. barnesiae*, including both morphotypes.
109 The measured parameters are the coccolith length (L) and width (W) in distal view, and the
110 inner cycle length (l) and width (w). In the Vergol section, 38 coccospheres were also
111 measured for their external and inner diameter and, when possible, the coccolith length was
112 also measured (Fig. 2b).

113

114 Figure 2 approx. here

115

116 A minimum of thirty coccoliths of *Watznaueria barnesiae* per sample were measured in 60
117 samples of the Vergol-La Charce composite section. Samples were collected from marl-
118 limestone couplets regularly distributed along the Vergol-La Charce composite section (Fig.
119 3). For the ODP Site 1149B, several samples were prepared but only 11 samples could be
120 analysed from the cores 16R to 27R, where the siliceous component is relatively limited and
121 nannofossils common (Fig. 4). Samples were prepared following the random settling
122 technique of Beaufort (1991) and Geisen et al. (1999), which ensures a homogeneous
123 dispersion of coccoliths on the slide. A small amount, 10 to 20 mg, of powdered rock was
124 diluted in 500 ml of water. After 24 hours of settling on the cover slide, the water was very
125 slowly evacuated, and turbulence was carefully avoided. Once dried, the cover slide was
126 mounted on a microscope slide using Rhodopass. This method ensures that coccoliths are
127 well isolated on the slide, they are not overlapping or tilted.

128 Images of at least 30 coccoliths per samples were taken under a LEICA DM750P, polarising
129 microscope at 1000X. Images were taken with a LEICA EC3 camera using the software LAS
130 (LEICA Application Suite). Measurements were done using ImageJ. The measurement
131 precision is $\pm 0.1 \mu\text{m}$, estimated by 30 repeated measurements of the calibration micrometre.
132 In the analysed images, $1 \mu\text{m}$ corresponds to 17.7 pixels. Measurement of 30 specimens per
133 sample is statistically robust when working on a single morphospecies (Suchéras-Marx et al.,
134 2010), because it gives a maximal error of 10% in the estimate of the mean (95% confidence
135 interval) and, with an increasing sample size (e.g., 50, 100 measurements or more), the error

136 percentage of the average value decreases very little. We applied the Suchéras-Marx et al.
137 (2010) test to our dataset, and we obtained similar results. Thus 30 specimens per sample
138 seem to be sufficient to evaluate the mean size of the population.

139 In addition to the length and width parameters, we have calculated the surface areas of the
140 inner and outer cycles of the coccolith, and its ellipticity (Figs. 3 and 4). Statistical analyses
141 have been then applied in order to test the robustness of the observed size trends. A
142 confidence interval at 95% of the average size values has been calculated as follows:

$$143 \text{CI}_{\text{average } (\alpha=0.5)} = 1.96 * (\sigma/\sqrt{N})$$

144 where σ is the standard deviation of the population, and N is the number of measured
145 specimens in each sample. Most of the statistical tests applied below need the analysed
146 data to be normally distributed. A Shapiro-Wilk test applied to our dataset shows that all the
147 samples have a normal distribution with $-2.7 \times 10^{-19} < p < 0.03$.

148

149 Figures 3 and 4 approx. here

150

151 2.1. Statistical treatment of biometric parameters

152

153 In order to test if there is a significant stratigraphical difference for the various parameters of
154 size analysed, an ANOVA (parametric ANalysis Of VAriance) was applied to the coccolith
155 length values of both sections using the software PAST. The null hypothesis is that all the
156 samples have the same average size values. We used the test of Levene, which analyses the
157 homogeneity of the variances and, when Levene was significant with a $p < 0.05$, the test F of
158 Welch was subsequently used. When the result of the test F of Welch was significant, the null
159 hypothesis could be rejected meaning that at least one sample differs significantly and non-
160 randomly from all the others.

161 Eventually, we have applied to the dataset the test of Tukey allowing comparison of samples
162 to each other for a given parameter and assessing the degree of similarity or, conversely, of
163 difference. This test is particularly useful for the Vergol-La Charce composite section, where
164 the number of samples is elevated. The percentage of the difference between groups made of
165 similar samples is then calculated. A MANOVA (Multivariate analysis of variance) was
166 applied, in order to assess the difference between the studied samples on the basis of four
167 parameters, namely L , W , l and w of *W. barnesiae* coccoliths.

168 A Run test was finally applied in order to assess the robustness of the observed trends of the

169 different size parameters. In this test, each value is compared to the median value with a null
170 hypothesis stating that the number of higher values is equal to the lower ones, thus there is not
171 a preferential trend. If the test is significant ($p < 0.05$) the null hypothesis can be rejected with
172 a risk α , which is calculated, and a significant trend is assessed.

173

174 2.2. Detection of modal trends in the analysed dataset

175

176 In order to discriminate between a uni- or a pluri-modal distribution of the analysed set of
177 data, and to identify the existence of one or more distinct groups within the totality of
178 coccolith length measurements, mixture analysis was applied to the Vergol-La Charce
179 measurements. This is a robust analysis tool performed with the software PAST, based on a
180 maximum-likelihood method. The minimum values of Akaike Information Criterion (AIC)
181 helped identifying the groups obtained by mixture analysis showing the lowest overfitting
182 (Hammer et al., 2001). The number of bins used for mixture analysis (8 in the present work,
183 0.5 μm each) depends on the size of the dataset and follows the Sturges' formula, as described
184 in Ferreira et al. (2017).

185

186 3. Results

187

188 3.1. Coccolith length versus coccosphere size

189

190 Coccolith length plotted *versus* coccolith width for the Vergol-La Charce composite section
191 and the ODP Site 1149B shows that these two parameters have a positive linear relationship
192 (Fig. 5a). Coccolith length varies at both sites from $\sim 3.1 \mu\text{m}$ to $7.7 \mu\text{m}$, coccolith width varies
193 from $2.6 \mu\text{m}$ to $6.5 \mu\text{m}$. In the following, we show coccolith length trends. Outer and inner
194 diameter of the coccosphere could be measured for 19 specimens (Fig. 5b). Coccospheres are
195 slightly elliptical and there is a very good coefficient of correlation between these two
196 parameters ($r=0.83$). The external diameter of the 38 coccospheres plotted *versus* the size of
197 their coccoliths shows that coccospheres vary between 6.5 and $12 \mu\text{m}$ (Fig. 5c), while
198 coccolith lengths are between 3.9 and $6.6 \mu\text{m}$. The coefficient of correlation between these
199 two parameters is 0.56 showing that, although coccolith size is dependent on the coccosphere
200 that produced it, there is a considerable degree of size variation.

201

202 Figure 5 approx. here

203

204 3.2. Coccolith size and shape through time

205

206 In the Vergol-La Charce section (Fig. 3), the size and the shape of *W. barnesiae* coccoliths
207 display long term changes. Average coccolith-length (L) fluctuates between 4.8 and 5.5 μm in
208 the upper Berriasian-lower Valanginian interval, until 44 m in the lower part of the NK 3A
209 nannofossil zone. In the same interval, coccolith ellipticity (E) attains some of the highest
210 values while the ratio between the surface of the coccolith and that of the inner cycle (S/s)
211 shows some of the lowest values. Average coccolith-length overall shows higher values with
212 weaker fluctuations in the upper part of lower Valanginian (upper part of the NK 3A zone)
213 and during the Weissert event (upper Valanginian), except for a single sample at 97 m with
214 very low values. Ellipticity is the lowest during the Weissert event with small fluctuations, the
215 S/s ratio is conversely quite high. Coccolith size is the highest in the uppermost Valanginian,
216 along with quite low ellipticity values and high S/s ratio.

217 This overall trend is confirmed by the Tukey test used for the contrast analysis which is based
218 on the results of the ANOVA. In synthesis, all the similar samples with a p value issued from
219 the Tukey test close to 1 have been grouped. Overall, 6 groups were recognized on the basis
220 of this variance analysis (right side of Fig. 3; Fig. 6a and b). The comparison of each of these
221 groups to the others allowed the calculation of the percentage of the difference between them
222 (Fig. 6b). The statistical difference between the samples belonging to these groups has been
223 then tested using a MANOVA (Fig. 6a). The samples are similar when the p -value is > 0.05 .
224 The smaller the p -value, the more different the samples. In synthesis, the samples at the base
225 of the section (groups 1 and 2) are significantly different from the samples corresponding to
226 the Weissert event and the interval above (groups 4 to 6). Group 3 (formed of a few samples)
227 represents a transition between the two other sets of samples.

228 ODP Site 1149B shows a pattern very similar to that of the Vergol-La Charce composite
229 section. Below the Weissert event *W. barnesiae* coccoliths show average lengths between 5
230 and 5.5 μm on average, are strongly elliptical and have weak values of S/s ratio. Coccolith
231 ellipticity is the lowest and the S/s ratio is the highest during the Weissert event. Size is the
232 highest with relatively weak ellipticity in the aftermath of the Weissert event.

233 For the ODP Site 1149B, the limited number of samples allowed a simpler data treatment.

234 When the Tukey test revealed a p -value < 0.05 , samples are significantly similar on the basis
235 of coccolith length (Fig. 6d). Thus, three groups of samples are identified: from 23R to 27R
236 spanning the lower Valanginian until the base of the Weissert event, from 20R to 22R in the

237 upper Valanginian, and from 16R to 19R uppermost Valanginian to lower Hauterivian.
238 However, the MANOVA analysis based on all the considered parameters (L, W, l and w of
239 *W. barnesiae* coccoliths) shows that samples 34R and 23R are significantly similar, thus 3
240 groups of samples are significantly different (Fig. 4 right side; Fig. 6c). So, the samples of
241 ODP Site 1149B corresponding to the Weissert event and just above display very peculiar
242 characters with respect to the other groups of samples located below and above the event
243 interval, and this pattern is very similar to that shown at Vergol-La Charce.

244

245 Figure 6 approx. here

246

247 3.3. *W. barnesiae* coccolith-size modes

248

249 The observed size shifts could be due to a variable mixture of larger and smaller species, this
250 is the reason why mixture analysis was applied. However, the minimum values of Akaike
251 Information Criterion (AIC) are obtained from mixture analysis when a unimodal distribution
252 is considered. A mode of 5.5 μm is observed (Fig. 7). As expected, similar results were
253 obtained when considering the coccolith width (data not shown). This suggests that only one
254 group of *W. barnesiae* occurs in terms of coccolith length, at least for the Vergol-La Charce
255 section in which a significant number of specimens could be measured.

256

257 Figure 7 approx. here

258

259 4. Discussion

260

261 4.1. Relationships between coccolith and coccosphere size

262

263 Fossil coccolithophore cell geometry and size allow detailed assessment of past cell
264 physiology and have important implications for the interpretation of coccolithophore-derived
265 biogeochemical palaeo-proxies that are affected by algal volume-to-surface area ratios (e.g.,
266 Henderiks and Pagani, 2007; Planq et al., 2012; Gibbs et al., 2013). Coccolith size is also a
267 useful proxy for calcite production and carbonate burial by coccolithophores (e.g., Young and
268 Ziveri, 2000; Suchéras-Marx et al., 2014). The relationship between coccolith size and
269 coccosphere size has never been explored in Mesozoic sediments, probably because of the
270 difficulty to recover entire coccospheres in ancient sediments, however this approach

271 represents a powerful tool to investigate coccolithophore cell geometry and size (Gibbs et al.,
272 2013).

273 The material we studied and, especially, the Vergol-La Charce samples provided us with the
274 possibility to analyse at the same time the coccosphere size and the coccoliths they hold. Our
275 results allow considerations on the coccosphere and cell dimensions and, when comparing our
276 results (Fig. 7) to the data shown by Henderiks (2008; fig. 3), *Watznaueria* displays a similar
277 relationship to that of typical Cenozoic coccoliths, suggesting that a change in mean coccolith
278 size most likely reflects a change in cell size. Unfortunately, the number of analysed
279 specimens is too low to establish a clear relationship between the coccolith and the
280 coccosphere size. In fact, in spite of a general positive correlation, the correlation coefficient
281 we record is relatively weak to establish a coccolith size rule as it was done for Cenozoic
282 genera (Henderiks, 2008). It is possible that besides the limited sampling size, our analyses
283 were hampered by the observations which were made under an optical microscope. Further
284 SEM analyses should be performed in order to better elucidate size rules for lower Cretaceous
285 coccoliths.

286

287 4.2. Significance of obtained results

288

289 Since the nineties, coccolith biometry has received a strong input and now represents a very
290 powerful proxy for paleoenvironmental interpretations, as well as for taxonomy and
291 evolution investigations. Most of the papers have shown bivariate graphs or frequency
292 distribution of simple parameters, such as coccolith length and width (e.g., Young, 1990;
293 Bornemann et al., 2003; Bornemann and Mutterlose, 2006; Linnert et al., 2014; Lübke et al.,
294 2015; Lübke and Mutterlose, 2016). Renaud et al. (2002) introduced the use of parametric
295 analysis of variance (ANOVA) in order to study the changes of morphological differences
296 and dynamics of the living coccolithophore *Calcidiscus leptoporus*. Barbarin et al. (2012)
297 used smoothing functions and tested the significance of the observed stratigraphical trends of
298 the nannolith *Nannoconus*. Giraud et al. (2006) have tested the relationships between various
299 biometric variables in the *Watznaueria britannica* pool using Principal Component Analysis.
300 Mixture analysis or Principal Component Analysis have been recently used to discriminate
301 between a uni- or pluri-modal distribution of size parameters (Suchéras-Marx et al., 2010;
302 Barbarin et al., 2012; Ferreira et al., 2017).

303 In this paper, following the guidelines of the Ferreira et al. (2017) paper, we have tested the
304 significance of the fluctuation of one (L) or more (L, W, l, w) parameters, using ANOVA and

305 MANOVA respectively. These different tests allowed us to identify groups of samples which
306 are significantly different from the others in the two studied localities. The general trend in
307 both studied sites is a significant size increase in the *W. barnesiae* coccolith length from ~5
308 μm to ~6.5 μm in the course of Valanginian. Slight differences between the two sites are very
309 likely due to a lower sample resolution in the ODP Site 1149B, making it difficult to precisely
310 assess the exact lower and upper boundary of the Weissert event.

311 Parallel to the size increase, morphology changed significantly across the Valanginian. In
312 both the studied sites, there is a general trend of decreasing ellipticity and increasing ϕ
313 coccolith-to-inner cycle ratio with the general increase of size. This is a known trend for
314 Cenozoic and extant species (*Pseudoemiliana lacunosa* or *Emiliana huxleyi*; Young, 1989;
315 Henderiks, 2008) and for upper Jurassic coccoliths (*W. britannica*; Giraud et al., 2006).
316 Biometry applied to these forms shows that larger coccoliths are globally less elliptical. This
317 constitutes an allometric trend and seems to indicate that the growth of coccoliths is more
318 effective for the minor axis, thus within a given genus larger coccoliths tend to be less
319 elliptical. However, the *W. barnesiae* specimens measured in this work display some of the
320 largest sizes in the aftermath of the Weissert event, where ellipticity is also significantly high.
321 It is therefore not excluded that besides the allometric trends in coccoliths, with ellipticity
322 decreasing along with size increase, peculiar environmental conditions occurring during the
323 Weissert event may have forced *W. barnesiae* to adopt a peculiar coccolith morphology.

324

325 4.3. Environmental versus evolutionary control on coccolith size and shape

326

327 In the literature, there is conspicuous evidence of micro-organism size changes during major
328 palaeoceanographic events. Significant size decrease is documented for coccoliths and
329 nannoliths during anoxic or hyperthermal events. This is the case for the Toarcian anoxic
330 event (T-OAE) where *Schizosphaerella* and coccoliths turned out to be smaller (Mattioli et
331 al., 2004; Suan et al., 2010), or the OAE1a where some coccolith species display
332 malformation and dwarfism (Erba et al., 2010; Lübke and Mutterlose, 2016). Conversely,
333 during the PETM interval the size of *Discoaster* increased in response to higher temperatures
334 and low nutrient concentrations in surface waters (Tremolada et al., 2012). Size and
335 calcification degree of coccoliths seem also to increase in response to arid conditions, likely
336 acting on the saturation state of oceanic surface-waters. This was the case for the late
337 Oxfordian (Giraud et al., 2006) or the Tithonian (Bornemann et al., 2003), but also for the
338 nannoconid recovery that occurred concomitant with the acme of the Weissert event (Barbarin

339 et al., 2012). The size of *W. barnesiae*, however, was evidently less sensitive to
340 environmental changes than that of other coccoliths. In fact, *W. barnesiae* size was not
341 significantly affected by environmental shifts during either OAE1a or OAE1d, leading the
342 authors to interpret it as having high environmental tolerance (Bornemann and Mutterlose,
343 2006; Lübke and Mutterlose, 2016). Also, no clear relationship exists between *W. barnesiae*
344 size patterns and proxies for palaeoenvironmental changes or geochemical cycling (Fig. 8),
345 although the size record is discontinuous in the Lower Cretaceous.

346 When comparing *W. barnesiae* size distribution data from the two sites considered in this
347 account located respectively in the Tethys (Vergol-La Chance) and in the Pacific (ODP Site
348 1149B), it is surprising to observe how closely both the bulk size distributions (Fig. 4) and the
349 Early Cretaceous size increase trend (Fig. 8) match in both sites. Analogous co-variation in
350 mean *Watznaueria* pool size were presented by Bornemann et al. (2003), who studied three
351 different oceanic sites of Tithonian to early Valanginian age, and by Erba et al. (2010) who
352 reported trends of *W. barnesiae* size in two sites in Tethys and Pacific Ocean during the
353 Aptian. These observations lead to two main deductions, namely that (i) the genetic flux was
354 not interrupted between populations in the Tethys and Pacific Oceans in the Lower
355 Cretaceous likely related to a circum-global circulation, and (ii) *Watznaueria* size trends are
356 more likely driven by supra-regional or evolutionary changes than by local environmental
357 conditions. We have compiled data on average coccolith length from various papers (Fig. 8),
358 and some peculiar patterns can be observed for the Cretaceous. Bornemann et al. (2003)
359 measured the *Watznaueria* pool, which is composed of *W. barnesiae*, *W. fossacincta*, *W.*
360 *britannica* and *W. manivittiae*, in three Atlantic sites. The average size per sample for this pool
361 was very high in the Tithonian (7-8 μm), then sharply decreased at the Jurassic/Cretaceous
362 boundary to around 5 μm in the mid-Berriasian. This shift corresponds to a drastic change in
363 the species-specific *Watznaueria* composition, large-sized forms of this genus (*W. cf.*
364 *manivittiae*, > 8 μm) were very abundant in the Tithonian, while *W. barnesiae* became
365 dominant within the genus by the Berriasian.

366

367 Figure 8 approx. here

368

369 The average size of ~5 μm measured in the upper Berriasian in three Atlantic sites by
370 Bornemann et al. (2003) corresponds thus to the record of the two sites (one in the Tethys and
371 the second in the Pacific) studied in this account. The most significant size increase of the *W.*
372 *barnesiae* pool occurred during the Valanginian and across the Weissert event, with average

373 sizes attaining $\sim 6.5 \mu\text{m}$. This size shift has turned out to be statistically significant and is
374 likely an example of Cope's rule, as already proposed for different marine microorganisms
375 (Schmidt et al., 2006) and for Jurassic coccolithophores (*Discorhabdus*, López-Otálvaro et
376 al., 2012; *Lotharingius*, Ferreira et al., 2017). Size evolution of the *W. barnesiae* lineage
377 seems to start near a limiting boundary ($\sim 5 \mu\text{m}$ on average), and then to diffuse away from an
378 originally small-sized ancestor, following the left-wall model (Stanley, 1973). In spite of a
379 discontinuous record of *W. barnesiae* size for the rest of the Cretaceous, it seems that average
380 sizes stayed quite stable in the aftermath of the Weissert event from late Valanginian until
381 Turonian, regularly fluctuating between ~ 5.5 to $\sim 6.5 \mu\text{m}$ or even lesser. Apparently, no
382 significant shifts occurred during the OAE 1b or Cenomanian/Turonian events (Bornemann
383 and Mutterlose, 2006; Linnert et al., 2014). During the OAE 1a, Erba et al. (2010) reported a
384 size decrease of *W. barnesiae* of about $1 \mu\text{m}$ from background values, which might attest for
385 the impact of palaeoceanographic changes, likely linked to increased $p\text{CO}_2$ levels, on
386 coccolith size (Fig. 8). However, size fluctuations of similar amplitude are also observed in
387 the Berriasian-Hauterivian interval, where a clear trend to size increase is observed.
388 *Watznaueria* radiated in times of elevated levels of $p\text{CO}_2$ (Fig. 8). Its resilience to periods of
389 enhanced $p\text{CO}_2$, like during the OAE 1a, might result from an “evolutionary memory” of past
390 atmospheric composition, as described for Cenozoic species by Henderiks and Rickaby
391 (2007).

392 *Watznaueria barnesiae* seems therefore to represent an example of directional selection, in
393 which a single extreme phenotype (in terms of size) is favoured (e.g., Kingsolver and Pfennig,
394 2004). The stationary model proposed by Stenseth and Maynard-Smith (1984), stating that
395 evolution is largely driven by abiotic changes such as temperature, water column stratification
396 or primary productivity does not seem to apply to the *W. barnesiae* size evolution, although
397 some extreme events (like OAE 1a) have produced a temporary size decrease. This model
398 conversely applies to other micro-organisms, as it is shown by the correlation observed
399 between size evolution of Cenozoic foraminifera and palaeoceanographic perturbations (Wei
400 and Kennett, 1983; Schmidt et al., 2004a, 2004b).

401 Although few measurements are available, *W. barnesiae* size seems to decrease to
402 background values from the Coniacian to Santonian (Fig. 8; *W. barnesiae* represents on
403 average $> 86\%$ of the *Watznaueria* pool measured by Linnert et al. (2014). This size decrease
404 started some 20 Myrs before the disappearance of the morpho-species which happened at the
405 end of the Cretaceous (Lees and Bown, 2005), although it sporadically occurred as a survivor
406 in basal Danian sediments (Bown, 2005).

407

408 **5. Conclusions**

409

410 *Watznaueria barnesiae* offers a unique opportunity to monitor the coccolith size and, to a
411 certain extent, the cell size over a very long time span, > 100 Myrs. The present paper focuses
412 on the upper Berriasian to basal Hauterivian interval, but comparisons with previous papers
413 allows considerations to be made for the whole Cretaceous period. This dominant and
414 eurytopic taxon is composed of at least two morphotypes (namely, *W. fossacincta* and *W.*
415 *barnesiae*) but, because of its longevity (~110 Myrs), it might be suspected to be composed of
416 a pool of cryptic species. If so, these are not distinguishable on the basis of biometric criteria,
417 because, as shown in this paper, the size distribution of *W. barnesiae* coccoliths is unimodal.
418 Whatever the genetic significance of this morpho-species, the coccolith size and shape are
419 remarkably similar in oceanic sites which are far away from each other, and subject to
420 different oceanographic regimes. This pattern seems to indicate that a genetic flux occurred
421 between populations in a context of a circum-global oceanic circulation.

422 The smallest size of *W. barnesiae* is recorded in the Berriasian with average values at around
423 5 μm . Then a statistically significant size increase is observed across the lower Valanginian,
424 starting before the palaeoceanographic Weissert event up to average values as high as 6.5 μm
425 in the uppermost Valanginian/basal Hauterivian. Coccolith size stayed then quite steady
426 oscillating between 5.5-6.5 μm from the Hauterivian to Turonian. No significant size changes
427 are observed in the middle Cretaceous apart from a temporary decrease during the OAE 1a,
428 although dramatic oceanic and climatic events occurred, such as the OAE 1a or the
429 Cenomanian/Turonian event. However, a decreasing size trend is observed from the
430 Coniacian.

431 Thus, the long-term pattern of the *W. barnesiae* coccolith size seems to be more likely related
432 to evolutionary trends than to a body-size response to drastic environmental changes.

433 *Watznaueria barnesiae* appears to have been a very robust taxon, poorly sensitive to
434 environmentally-driven changes, as far as its coccolith size is concerned. Although we do not
435 have any detailed size record data for the Jurassic period, which witnesses the rise to
436 dominance of this taxon within the nannofossil assemblage, *W. barnesiae* lineage seems to
437 follow Cope's rule in the Berriasian-Barremian interval, which is the tendency for lineages to
438 evolve to larger body size. In this regard, *W. barnesiae* displays a certain similarity with the
439 Jurassic genus *Lotharingius* also belonging to the Watznaueriaceae (Ferreira et al., 2017).

440 *Watznaueria barnesiae* size changes seem therefore to illustrate a directional selection, in

441 which a single extreme phenotype (in terms of size) is favored through time, then returning to
442 smaller size during its late stratigraphic range. If this model held true, then due to the
443 dominance of this taxon in Mesozoic rocks, *W. barnesiae* size could be used in future works
444 along with quantification of its export fluxes for assessing the transfer of particulate inorganic
445 and organic carbon to the sedimentary reservoirs, thus implementing biogeochemical
446 modelling.

447

448 **Acknowledgements**

449

450 We wish to warmly thank Dr. Gilles Escarguel, whose discussions with B.G. were very
451 inspiring. This research was supported by the INSU TelluS-INTERRVIE and IODP France
452 (Post-Cruise funding) to E.M. Smear slides are curated at the Collections de Géologie de
453 Lyon (FSL N° 766104-766186). Valuable comments from two anonymous reviewers and by
454 Ric Jordan greatly improved the overall quality of this manuscript.

455

456 **Reference list**

457

458 Aloisi, G., 2015. Co-variation of metabolic rates and cell-size in coccolithophores.

459 *Biogeosciences Discussions*, 12(8), 6215–6284.

460 Atkinson, D., Ciotti, B.J., Montagnes, D.J., 2003. Protists decrease in size linearly with

461 temperature: ca. 2.5% C⁻¹. *Proceedings of the Royal Society of London B: Biological*
462 *Sciences*, 270(1533), 2605–2611.

463 Barbarin, N., Bonin, A., Mattioli, E., Pucéat, E., Cappetta, H., Gréselle, B., Pittet, B., Vennin,

464 E., Joachimski, M., 2012. Evidence for a complex Valanginian nannoconid decline in
465 the Vocontian basin (South East France). *Marine Micropaleontology*, 84, 37–53.

466 Beaufort, L., Probert, I., de Garidel-Thoron, T., Bendif, E.M., Ruiz-Pino, D., Metzl, N.,

467 Goyet, C., Buchet, N., Coupel, P., Grelaud, M., Rost, B., Rickaby, R.E.M., de Vargas,
468 C., 2011. Sensitivity of coccolithophores to carbonate chemistry and ocean

469 acidification. *Nature* 476 doi:10.1038/nature10295

470 Berner, R.A., 2004. *The Phanerozoic Carbon Cycle: CO₂ and O₂*. Oxford University Press,

471 159 pp.

472 Bornemann, A., Aschwer, U., Mutterlose, J., 2003. The impact of calcareous nannofossils on
473 the pelagic carbonate accumulation across the Jurassic–Cretaceous boundary.

474 *Palaeogeography, Palaeoclimatology, Palaeoecology*, 199(3–4), 187–228.

- 475 Bornemann, A., Mutterlose, J., 2006. Size analyses of the coccolith species *Biscutum*
476 *constans* and *Watznaueria barnesiae* from the Late Albian « Niveau Breistroffer » (SE
477 France): taxonomic and palaeoecological implications. *Geobios*, 39(5), 599–615.
- 478 Bown, P.R., 2005. Selective calcareous nannoplankton survivorship at the Cretaceous–
479 Tertiary boundary. *Geology* 33, 653–656.
- 480 Erba, E., Tremolada, F., 2004. Nannofossil carbonate fluxes during the Early Cretaceous:
481 phytoplankton response to nutrification episodes, atmospheric CO₂ and anoxia.
482 *Paleoceanography* 19. doi:10.1029/2003PA000884.
- 483 Erba, E., Bartolini, A., Larson, R.L., 2004. Valanginian Weissert oceanic anoxic event.
484 *Geology* 32, 149– 152.
- 485 Erba, E., Bottini, C., Weissert, H.J., Keller, C.E., 2010. Calcareous Nannoplankton Response
486 to Surface-Water Acidification Around Oceanic Anoxic Event 1a. *Science* 329, 428-
487 432.
- 488 Ferreira, J., Mattioli, E., van de Schootbrugge, B. (2017). Palaeoenvironmental vs.
489 evolutionary control on size variation of coccoliths across the Lower-Middle Jurassic,
490 *Palaeogeography, Palaeoclimatology, Palaeoecology*,
491 <http://dx.doi.org/10.1016/j.palaeo.2016.10.029>
- 492 Finkel, Z.V., Beardall, J., Flynn, K.J., Quigg, A., Rees, T.A.V., Raven, J.A., 2009.
493 Phytoplankton in a changing world: cell size and elemental stoichiometry. *Journal of*
494 *Plankton Research*, fbp098.
- 495 Föllmi, K. B., 2012. Early Cretaceous life, climate and anoxia. *Cretaceous Research*, 35, 230–
496 257.
- 497 Fu, F.-X., Mulholland, M.R., Garcia, N.S., Beck, A., Bernhardt, P.W., Warner, M.E., Sañudo,
498 S.A., Hutchins, D.A., 2008. Interactions between changing *p*CO₂, N₂ fixation, and Fe
499 limitation in the marine unicellular cyanobacterium *Crocospaera*. *Limnology and*
500 *Oceanography*, 53(6), 2472–2484.
- 501 Gibbs, S.J., Poulton, A.J., Bown, P.R., Daniels, C.J., Hopkins, J., Young, J.R., Jones, H.L.,
502 Thiemann, G.J., O’Dea, S.A., Newsam, C., 2013. Species-specific growth response of
503 coccolithophores to Palaeocene–Eocene environmental change. *Nature Geoscience* 6,
504 218-222.
- 505 Giraud, F., Pittet, B., Mattioli, E., Audouin, V., 2006. Paleoenvironmental controls on the
506 morphology and abundance of the coccolith *Watznaueria britannica* (Late Jurassic,
507 southern Germany). *Marine Micropaleontology* 60(3), 205–225.

508 Gradstein, F.M., Ogg, J.G., Schmitz, M., Ogg, G., 2012. The Geologic Time Scale 2012.
509 Published by Elsevier B.V. DOI: 10.1016/B978-0-444-59425-9.00001-9

510 Gréselle, B., Pittet, B., Mattioli, E., Joachimski, M., Barbarin, N., Riquier, L., Reboulet, S.,
511 Pucéat, E. (2011). The Valanginian isotope event: A complex suite of
512 palaeoenvironmental perturbations. *Palaeogeography, Palaeoclimatology,*
513 *Palaeoecology* 306/1-2, 41-57. doi: 10.1016/j.palaeo.2011.03.027

514 Hammer, Ø., Harper, D.A.T., Ryan, P.D., 2001. PAST: paleontological statistics software
515 package for education and data analysis. *Palaeontol. Electron.* 4, 1–9.

516 Henderiks, J., 2008. Coccolithophore size rules—reconstructing ancient cell geometry and
517 cellular calcite quota from fossil coccoliths. *Marine Micropaleontology*, 67(1), 143–
518 154.

519 Henderiks, J., Pagani, M., 2007. Refining ancient carbon dioxide estimates: Significance of
520 coccolithophore cell size for alkenone-based $p\text{CO}_2$ records. *Paleoceanography* 22,
521 PA3202, doi:10.1029/2006PA001399, 2007

522 Hopkins, J., Henson, S.A., Painter, S.C., Tyrrell, T., Poulton, A.J., 2015. Phenological
523 characteristics of global coccolithophore blooms, *Global Biogeochem. Cycles*, 29,
524 doi:10.1002/2014GB004919.

525 Iglesias-Rodriguez, M.D., Halloran, P.R., Rickaby, R.E.M., Hall, I.R., Colmenero-Hidalgo,
526 E., Gittins, J.R., Green, D.R.H., Tyrrell, T., Gibbs, S.J., von Dassow, P., Rehm, E.,
527 Armbrust, E.V., Boessenkohl, K.P., 2008. Phytoplankton calcification in a High- CO_2
528 World. *Science* 320, 336–340.

529 Kenjo, S., 2014. Biostratigraphie intégrée à nannofossiles calcaires et ammonoïdes :
530 développement et implications pour la définition et la valorisation des stratotypes
531 d'unité et de limite. L'exemple des étages Berriasien et Valanginien et de leur limite
532 (140 Millions d'années) (Unpubl. PhD thesis). University of Lyon-1, 226 pp.

533 Kenjo, S., Mattioli, E., Reboulet, S., Bert, D., Ma'Louleh, K., 2013. Integrated
534 Biostratigraphy of Calcareous Nannofossils and Ammonoids. Implications for the
535 Definition of the Stratotype of the Berriasian–Valanginian Boundary (139.4 Ma). In:
536 Rocha, R., Pais, J., Kullberg, J.C., Finney, S. (Eds), *STRATI 2013 First International*
537 *Congress on Stratigraphy*, Springer, 261-266 pp.

538 Key, T., McCarthy, A., Campbell, D.A., Six, C., Roy, S., Finkel, Z.V., 2010. Cell size trade-
539 offs govern light exploitation strategies in marine phytoplankton. *Environmental*
540 *microbiology* 12(1), 95–104.

541 Kingsolver, J.G., Pfennig, D.W., July 2004. Individual-level selection as a cause of Cope's
542 rule of phyletic size increase. *Evolution* 58(7), 1608–1612. doi:10.1554/04-003. PMID
543 15341162.

544 Lees, J.A., Bown, P.R., 2005. Upper Cretaceous calcareous nannofossil biostratigraphy, ODP
545 Leg 198 (Shatsky Rise, northwest Pacific Ocean). In Bralower, T.J., Premoli Silva, I.,
546 and Malone, M.J. (Eds.), *Proc. ODP, Sci. Results, 198: College Station, TX (Ocean
547 Drilling Program)*, 1–60. doi:10.2973/odp.proc.sr.198.114.

548 Lees, J. A., Bown, P. R., Mattioli, E., 2005. Problems with proxies? Cautionary tales of
549 calcareous nannofossil paleoenvironmental indicators. *Micropaleontology*, 51(4),
550 333-343.

551 Lewis, W. M., 1976. Surface/volume ratio: implications for phytoplankton morphology.
552 *Science*, 192(4242), 885-887.

553 Lini, A., Weissert, H., and Erba, E., 1992. The Valanginian carbon isotope event: A first
554 episode of greenhouse climate conditions during the Cretaceous. *Terra Nova* 4, 374–
555 384.

556 Linnert, C., Mutterlose, J., Bown, P.R., 2014. Biometry of Upper Cretaceous (Cenomanian–
557 Maastrichtian) coccoliths – a record of long-term stability and interspecies size shifts.
558 *Revue de micropaléontologie* 57, 125–140.

559 López-Otálvaro, G.E., Suchéras-Marx, B., Giraud, F., Mattioli, E., Lécuyer, C., 2012.
560 *Discorhabdus* as a key coccolith genus for paleoenvironmental reconstructions (Middle
561 Jurassic, Lusitanian Basin): Biometry and taxonomic status. *Marine Micropaleontology*
562 94–95, 45–57.

563 Lozar, F., Tremolada, F., 2003. Calcareous nannofossil biostratigraphy of Cretaceous
564 sediments recovered at ODP Site 1149 (Leg 185, Nadezhda Basin, western Pacific). In
565 Ludden, J.N., et al., *Proceedings of the Ocean Drilling Program, Scientific results,*
566 *Volume 185 (online):* <http://www.odp.tamu.edu/publications/185pSR/010/010.htm>.

567 Lübke, N., Mutterlose, J., 2016. The impact of OAE 1a on marine biota deciphered by size
568 variations of coccoliths. *Cretaceous Research* 61, 169-179.

569 Lübke, N., Mutterlose, J., Bottini, C., 2016. Size variations of coccoliths in Cretaceous oceans
570 — A result of preservation, genetics and ecology? *Marine Micropaleontology* 117, 25–
571 39.

572 Mattioli, E., Erba, E., 1999. Biostratigraphic synthesis of calcareous nannofossil events in the
573 Tethyan Jurassic. *Rivista Italiana di Paleontologia e Stratigrafia* 105(3), 343-376.

- 574 Mattioli, E., Pittet, B., Young, J.R., Bown, P.R., 2004. Biometric analysis of Pliensbachian-
575 Toarcian (Lower Jurassic) coccoliths of the family Biscutaceae: intra- and interspecific
576 variability versus palaeoenvironmental influence. *Marine Micropalaeontology* 52, 5-27.
- 577 Mattioli, E., Pittet, B., Riquier, L., Grossi, V., 2014. The mid-Valanginian Weissert Event as
578 recorded by calcareous nannoplankton in the Vocontian Basin. *Palaeogeography,*
579 *Palaeoclimatology, Palaeoecology* 414, 472-485.
- 580 Mutterlose, J., Bornemann, A., Herrle, J.O., 2005. Mesozoic calcareous nannofossils — state
581 of the art. *Paläontol. Z.* 79, 113–133.
- 582 Plancq, J., Grossi, V., Henderiks, J., Simon, L., Mattioli, E., 2012. Alkenone producers during
583 late Oligocene–early Miocene revisited. *Paleoceanography* 27, PA1202,
584 doi:10.1029/2011PA002164, 2012
- 585 Plank, T., Ludden, J. N., Escutia, C. et al, 2000. Leg 185 summary; inputs to the Izu–Mariana
586 subduction system. *Ocean Drilling Program Proceedings, Initial Reports, Leg, 185,* 1–
587 63.
- 588 Popp, B.N., Laws, E.A., Bidigare, R.R., Dore, J.E., Hanson, K.L., Wakeham, S.G., 1998.
589 Effect of phytoplankton cell geometry on carbon isotopic fractionation, *Geochim.*
590 *Cosmochim. Acta,* 62, 69–77, doi:10.1016/S0016-7037(97)00333-5.
- 591 Reboulet, S., 1996. L'évolution des ammonites du Valanginien-Hauterivien inférieur du
592 bassin vocontien et de la plate-forme provençal (Sud-Est de la France): relations avec la
593 stratigraphie séquentielle et implications biostratigraphiques. *Documents des*
594 *Laboratoires de Géologie de Lyon* 137 (1995), 371 pp.
- 595 Reboulet, S., Atrops, F., 1999. Comments and proposals about the Valanginian-Lower
596 Hauterivian ammonite zonation of south-east France. *Eclogae geologicae Helvetiae* 92,
597 183-197.
- 598 Reboulet, S., Rard, A., 2008. Double alignments of ammonoid aptychi from the Lower
599 Cretaceous of Southeast France: Result of a post-mortem transport or bromalites? *Acta*
600 *Palaeontologica Polonica* 53(2), 261–274.
- 601 Reboulet, S., Mattioli, E., Pittet, B., Baudin, F., Olivero, D., Proux, O., 2003. Ammonoid and
602 nannoplankton abundance in Valanginian (early Cretaceous) limestone–marl
603 successions from the southeast France Basin: carbonate dilution or productivity?
604 *Palaeogeography, Palaeoclimatology, Palaeoecology,* 201(1), 113–139.
- 605 Reboulet, R., Szives, O., Aguirre-Urreta, B., Barragán, R., Company, M., Idakieva, V.,
606 Ivanov, M., Kakabadze, M.V., Moreno-Bedmar, J.A., Sandoval, J., Baraboshkin, E.J.,
607 Çaglar, M.K., Fözy, González-Arreola, C., Kenjo, S., Lukeneder, A., Raisossadat, S.N.,

608 Rawson, P.F., Tavera, J.M., 2014. Report on the 5th International Meeting of the IUGS
609 Lower Cretaceous Ammonite Working Group, the Kilian Group (Ankara, Turkey, 31st
610 August 2013). *Cretaceous Research* 50, 126-137.

611 Reboulet, S., Szives, O. (reporters), Aguirre-Urreta, B., Barragán, R., Company, M., Frau, C.,
612 Kakabadze, M.V., Klein, J., Moreno-Bedmar, J.A., Lukeneder, A., Pictet, P., Ploch, I.,
613 Raisossadat, S.N., Vašíček, Z., Baraboshkin, E.J., Mitta, V.V., 2018. Report on the 6th
614 International Meeting of the IUGS Lower Cretaceous Ammonite Working Group, the
615 Kilian Group (Vienna, Austria, 20th August 2017). *Cretaceous Research* 91: 100–110.

616 Renaud, S., Ziveri, P., Broerse, A.T.C., 2002. Geographical and seasonal differences in
617 morphology and dynamics of the coccolithophore *Calcidiscus leptoporus*. *Mar.*
618 *Micropaleontol.* 46, 363– 385.

619 Riebesell, U., Zondervan, I., Rost, B., Tortell, P.D., Zeebe, R.E., Morel, F.M.M., 2000.
620 Reduced calcification of marine plankton in response to increased atmospheric CO₂.
621 *Nature* 407, 364–367.

622 Roth, P.H., Krumbach, K.R., 1986. Middle Cretaceous calcareous nannofossil biogeography
623 and preservation in the Atlantic and Indian oceans: implications for paleoceanography.
624 *Mar. Micropaleontol.* 10, 235–266.

625 Schmidt, D.N., Thierstein, H.R., Bollmann, J., 2004a. The evolutionary history of size
626 variation of planktic foraminiferal assemblages in the Cenozoic. *Palaeogeography,*
627 *Palaeoclimatology, Palaeoecology* 212, 159–180.

628 Schmidt, D.N., Thierstein, H.R., Bollmann, J., Schiebel, R., 2004b. Abiotic forcing of
629 plankton evolution in the Cenozoic. *Science* 303, 207–210.

630 Stanley, S.M., 1973. An explanation for Cope's rule. *Evolution* 27, 1–26.

631 Suan, G., Mattioli, E., Pittet, B., Lécuyer, C., Suchéras-Marx, B., Duarte, L.V., Philippe, M.,
632 Reggiani, L., Martineau, F., 2010. Secular environmental precursors to Early Toarcian
633 (Jurassic) extreme climate changes. *Earth and Planetary Science Letters* 290, 448–458.

634 Suchéras-Marx, B., Mattioli, E., Pittet, B., Escarguel, G., Suan, G., 2010. Astronomically-
635 paced coccolith size variations during the early Pliensbachian (Early Jurassic).
636 *Palaeogeography, Palaeoclimatology, Palaeoecology* 295(1), 281–292.

637 Suchéras-Marx, B., Giraud, F., Mattioli, E., Gally, Y., Barbarin, N., Beaufort, L. (2014).
638 Middle Jurassic coccolith fluxes: A novel approach by automated quantification.
639 *Marine Micropaleontology* 111, 15–25

640 Tremolada, F., De Bernardi, B., Erba, E., 2012. Size variations of the calcareous nannofossil
641 taxon *Discoaster multiradiatus* (*Incertae sedis*) across the Paleocene–Eocene thermal

642 maximum in ocean drilling program holes 690B and 1209B. *Marine Micropaleontology*
643 67, 239–254.

644 Wei, K.-Y., Kennett, J.P., 1983. Nonconstant extinction rates of Neogene planktonic
645 foraminifera. *Nature* 305, 218–220.

646 Young, J.R., 1989. Observations on heterococcolith rim structure and its relationship to
647 developmental processes. In: Crux, J.A., van Heck, S.E. (Eds.), *Nannofossils and their*
648 *applications*. Ellis Horwood, Chichester, pp. 1–20

649 Young, J.R., 1990. Size variation of Neogene *Reticulofenestra* coccoliths from Indian Ocean
650 DSDP Cores. *J. Micropaleontol.* 9, 71– 86.

651 Young, J.R., Ziveri, P., 2000. Calculation of coccolith volume and its use in calibration of
652 carbonate flux estimates. *Deep-Sea Research II* 47, 1679-1700.

653 Zella, P., Stinnesbeck, W., Beckmann, S., Adatte, T., Heringa, F., 2015. The Berriasian–
654 Valanginian (Early Cretaceous) boundary transition at Santa Catarina Ticuá, Oaxaca
655 state, southern Mexico: Ammonites, bivalves, calpionellids and their
656 paleobiogeographic significance. *Journal of South American Earth Sciences* 62, 33-57.

657

658 **Figure legend**

659

660 Figure 1. (a) Global palaeogeographic map for the lower Cretaceous, redrawn from Zella et
661 al. (2015), where the approximate position of the two studied sites is shown. (b) In the
662 lower Cretaceous, the epicontinental Vocontian Basin was surrounded by shallow-
663 carbonate platforms and was opened to the Tethys Ocean to the East (after Gréselle et
664 al., 2011). (c) The ODP Site 1149B was located in the western Pacific Ocean, Nadezhda
665 Basin.

666 Figure 2. (a) Micrograph of a *W. barnesiae* coccolith in optical microscope, crossed polars.
667 The measured parameters are shown, namely: coccolith length (L) and width (W), and
668 inner-cycle length (l) and width (w). (b) Coccosphere of *W. barnesiae* in optical
669 microscope (parallel polars) with the parameters which were measured, namely the
670 outer and inner diameter of the coccosphere and, when possible the coccoliths forming
671 it.

672 Figure 3. Vergol-La Charce composite section. Average coccolith length per sample with
673 95% confidence interval, average coccolith ellipticity and average ratio coccolith/inner
674 cycle surface. The stratigraphic patterns of these biometric parameters are plotted
675 against the stratigraphic column (after Gréselle et al., 2011), the age, and the $\delta^{13}\text{C}_{\text{bulk}}$

676 values. The ammonite zonation is built after Reboulet (1996), Reboulet and Atrops
677 (1999), Reboulet and Rard (2008), Kenjo (2014), and updated according to the standard
678 zonation established by Reboulet et al. (2014; 2018). Abbreviated ammonite names are:
679 Inostr. = Inostranzewi; Platy. = Platycostatus; Proneco. = Pronecostatum; Callid. =
680 Callidiscus. The position of organic matter-rich levels, the Barrande layers (Reboulet et
681 al., 2003), and of the Weissert event are shown by shaded areas. On the right side of the
682 figure are shown the groups of samples that are significantly different based on
683 statistical analyses applied to the measured parameters.

684 Figure 4. ODP Site 1149B. Average coccolith length per sample with 95% confidence
685 interval, average coccolith ellipticity and average ratio coccolith/inner cycle surface.
686 The stratigraphic patterns of these biometric parameters are plotted against cores,
687 lithology, age model, and the $\delta^{13}\text{C}_{\text{bulk}}$ values (after Plank et al., 2000). The position of
688 the Weissert event is shown by shaded area. On the right side of the figure are shown
689 the groups of samples that are significantly different based on statistical analyses
690 applied to the measured parameters.

691 Figure 5. (a) Bivariate plot of *W. barnesiae* coccolith length versus width for the two studied
692 sites. The two shown parameters have a positive linear relationship. (b) The plot of
693 outer versus inner diameter for 19 measured **coccospheres** shows a very significant
694 coefficient of correlation ($r = 0.83$). (c) When plotting coccosphere outer diameter
695 versus the coccolith length measured on the coccospheres, the correlation coefficient is
696 positive but data show a certain dispersion.

697 Figure 6. (a) The statistical difference between the samples belonging to the different groups
698 has been tested using a MANOVA. The samples are similar when the p -value is > 0.05 .
699 The smaller the p -value, the more different the samples are. (b) Eventually, the
700 percentage of difference between the 6 recorded groups has been tested. See the text for
701 more explanation. (c). The samples were directly compared to each other using a
702 MANOVA. Samples are statistically different when p is lower than 0.05. The lower the
703 p -values, the higher is the difference between samples. (d) Solid lines show the groups
704 of samples that are statistically different from each other.

705 Figure 7. Results of the mixture analysis applied to the 1918 *W. barnesiae* specimens
706 measured in the Vergol-La Charce section (coccolith length). The minimum values of
707 Akaike Information Criterion (AIC) helped to detect the groups obtained by mixture
708 analysis which show the lowest overfitting. For the studied dataset, a uni-modal
709 distribution provided the lowest AIC values. The number of bins used for mixture

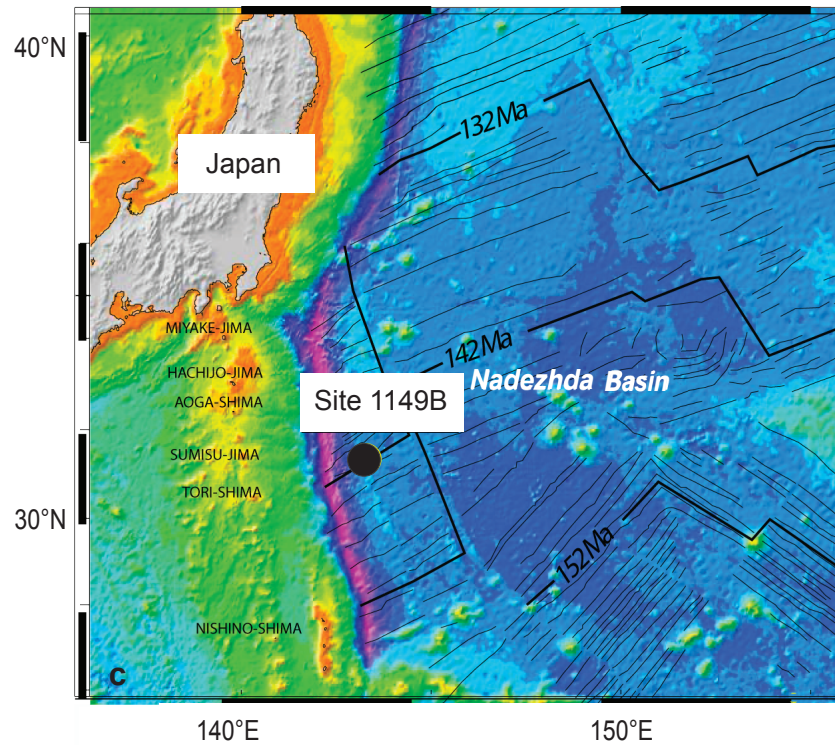
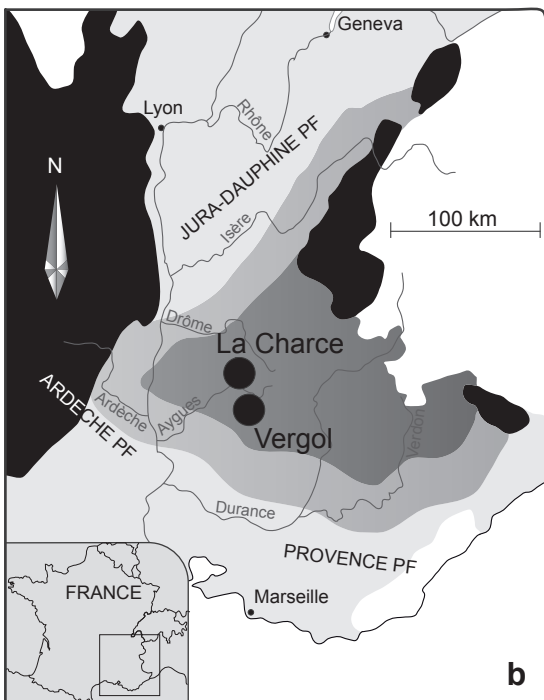
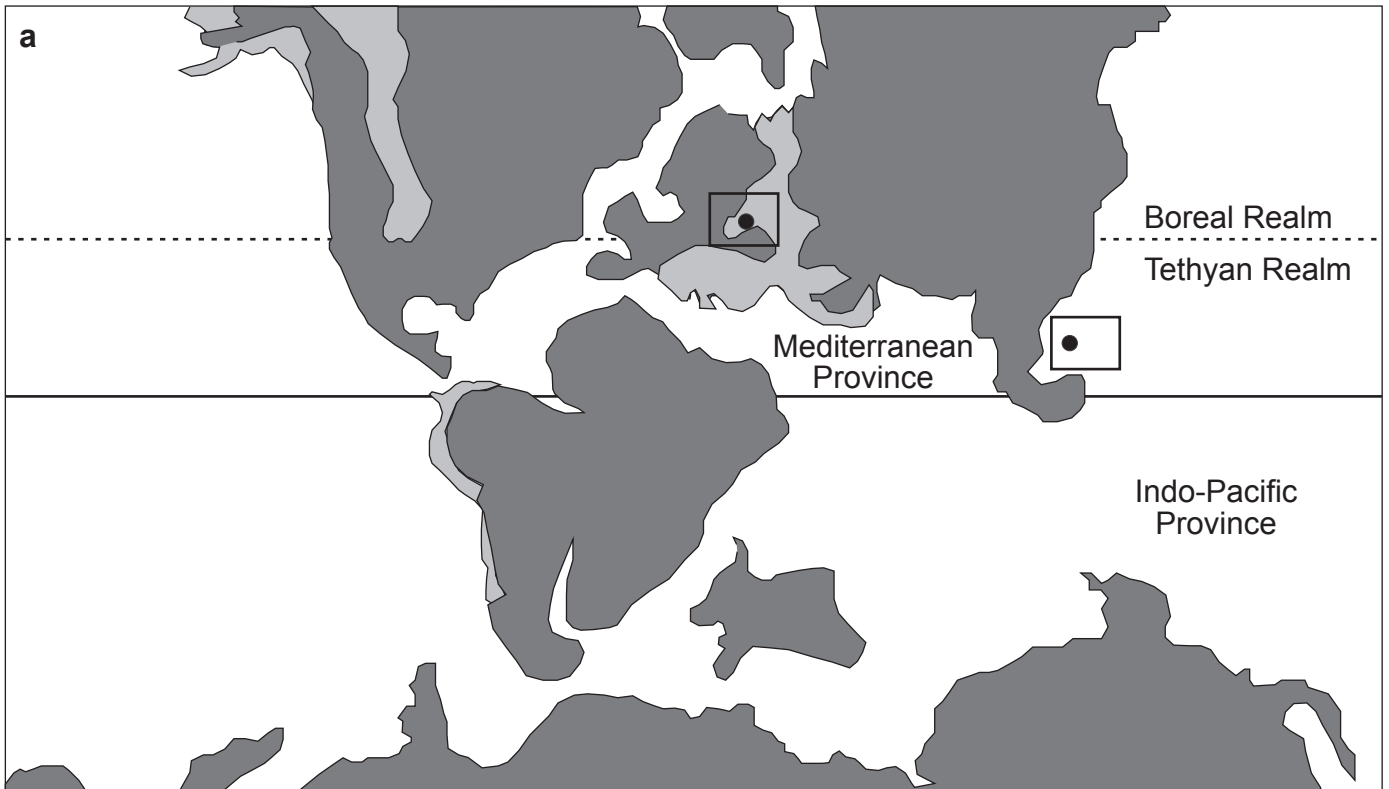
710 analysis (8 in the present work, 0.5 μm each) has been chosen according to the Sturges'
711 formula (Ferreira et al., 2017). The modal value is 5.5 μm .

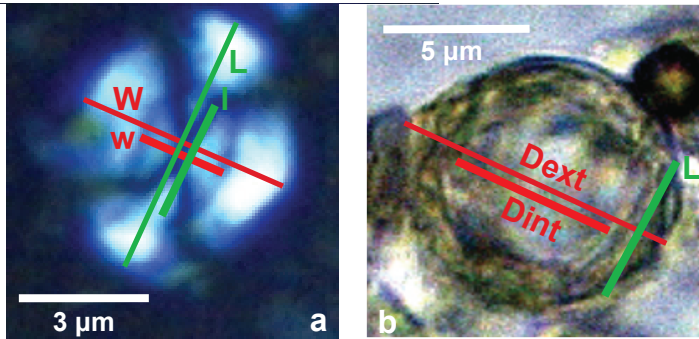
712 Figure 8. Average values per sample of *W. barnesiae* coccolith-length as deduced from this
713 study (grey lines) and from the literature. First and last occurrence datums of *W.*
714 *barnesiae* are shown. Also, the stratigraphic position of the most significant
715 palaeoceanographic events of the Mesozoic is displayed (shaded lines). Please, note that
716 the sharp size decrease in size reported by Bornemann et al. (2003) and occurring at the
717 Tithonian-Berriasian is mainly related to a species-specific change. The *Watznaueria*
718 pool contained less than 50% of *W. barnesiae* in the Tithonian, but more than 90% in
719 the Berriasian. The Berriasian sizes documented by Bornemann et al. (2003) are thus
720 mainly related to *W. barnesiae*. Also for the upper Cretaceous sizes, Linnert et al.
721 (2014) measured all the *Watznaueria* pool. However, this is largely dominated (more
722 than 86%) by *W. barnesiae*. The observed size trend is thus mainly related to *W.*
723 *barnesiae* size fluctuations. The $^{87}\text{Sr}/^{86}\text{Sr}$ mean LOWESS fitted line through the data is
724 after Gradstein et al. (2012). The $\delta^{13}\text{C}_{\text{carb}}$ curve is after the compilation of Gradstein et
725 al. (2012). The $\delta^{18}\text{O}$ curves resulted from belemnite calcite or from planktonic
726 foraminifers (for the Campanian-Maastrichtian interval in tropical, subtropical regions),
727 according to the compilation of Gradstein et al. (2012). Error bars show the 90%
728 confidence envelope. For the temperature scale, see Gradstein et al. (2012). The
729 reconstruction of the atmospheric CO_2 in the considered time span is redrawn from
730 Berner (2004). Black boxes on the right side show the ages of the Large Igneous
731 Province emplacement (Gradstein et al., 2012): Karoo-Ferrar, at ~183 Ma; Parana-
732 Etendeka, at ~136-133 Ma; Ontong Java Plateau-Manihiki Plateau, at ~125-123 Ma;
733 Kerguelen Plateau-Rajmahal Traps, at ~118 Ma; Caribbean-Columbian Province, at ~90
734 Ma; Deccan Traps, at ~66-65 Ma.

735

736

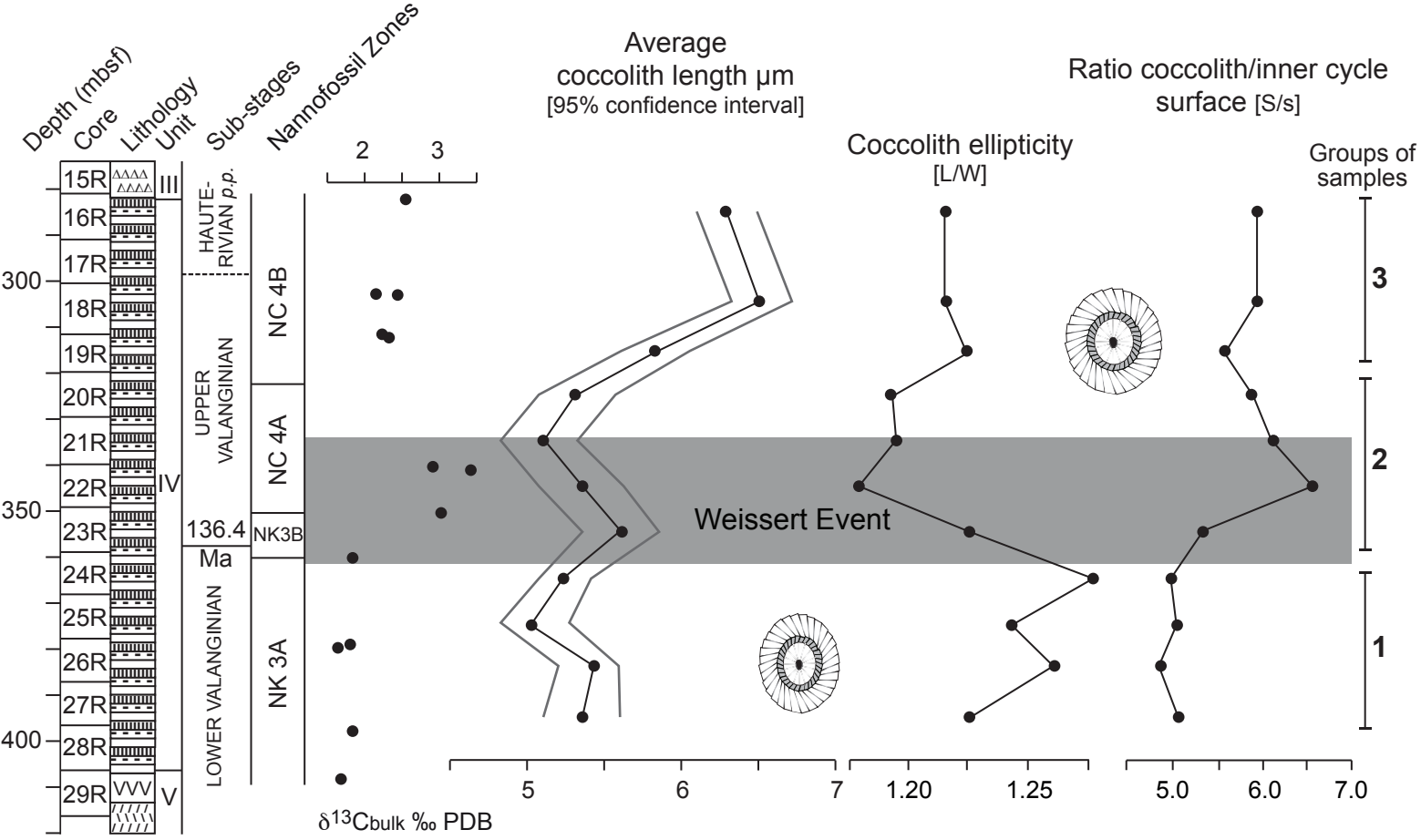
737





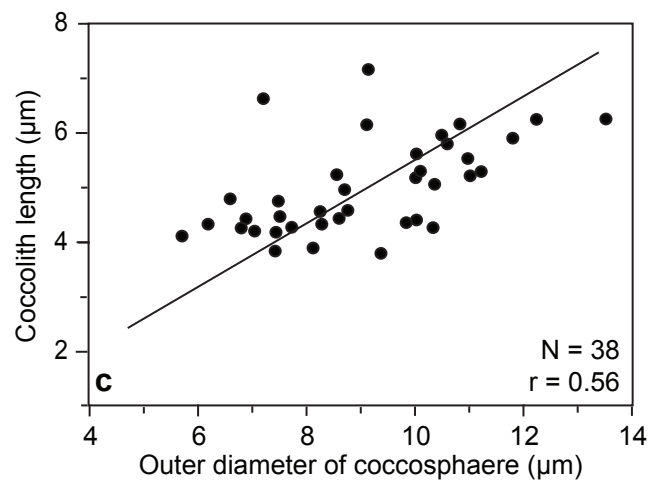
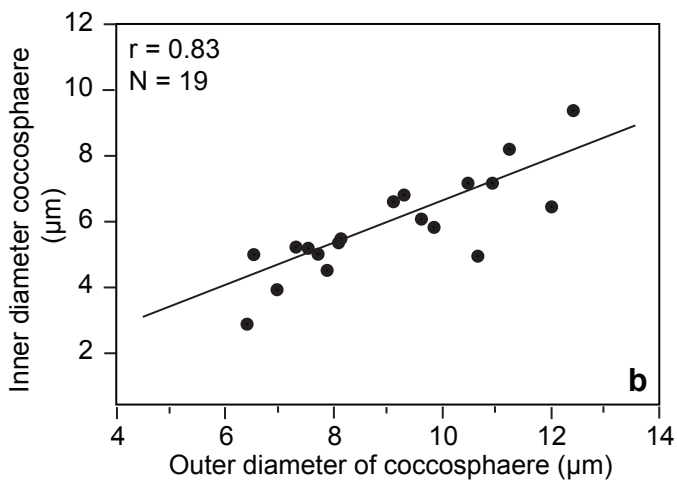
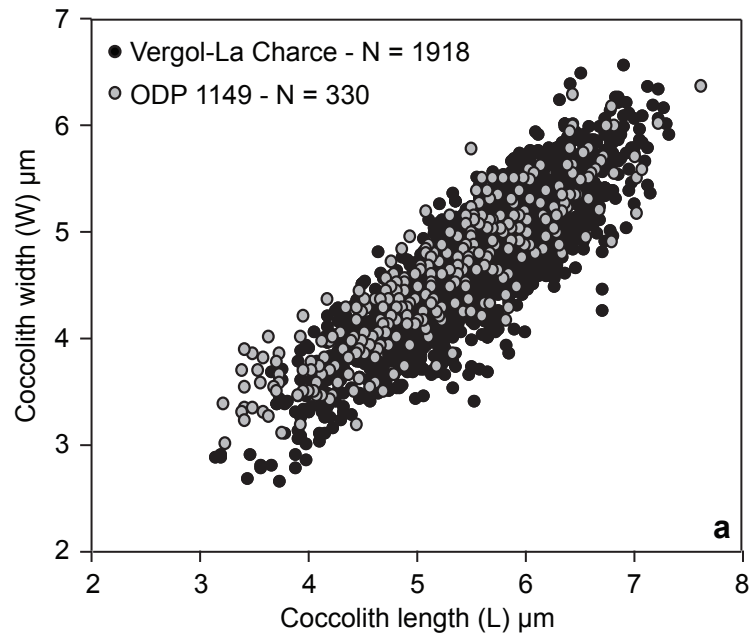
Gollain et al. Figure 2

ODP SITE 1149B



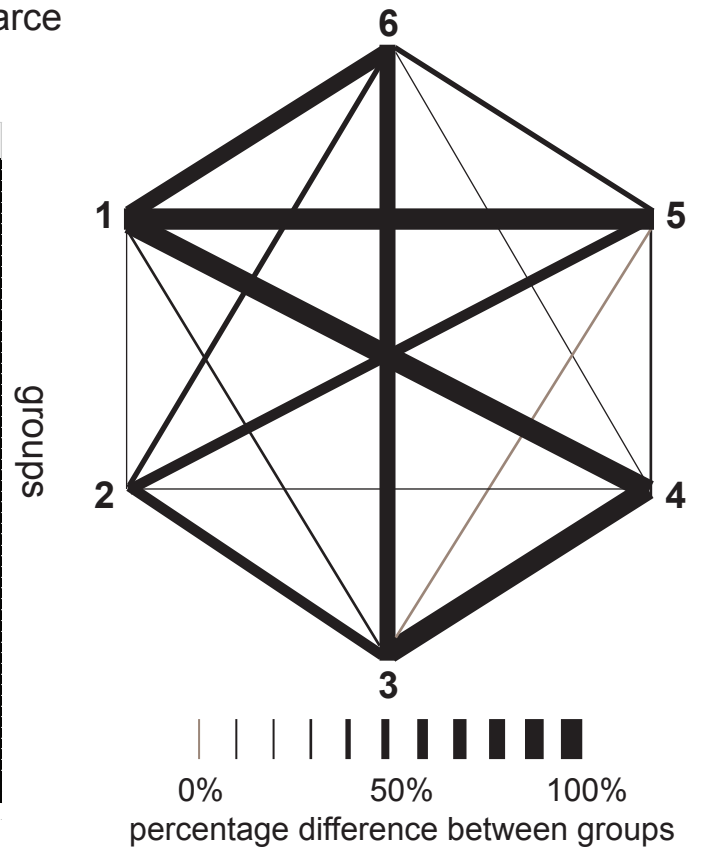
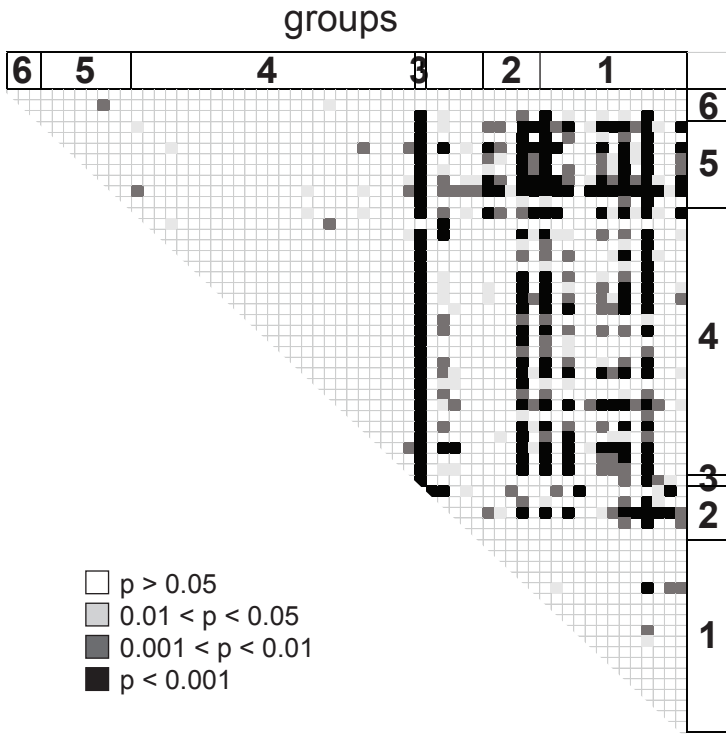
Unit III: interbedded radiolarian chert, porcellanite and siliceous clay
 Unit IV: interbedded radiolarian chert and radiolarian/nanofossil chalk/marl
 Unit V: basalt

Gollain et al. Figure 4



Gollain et al. Figure 5

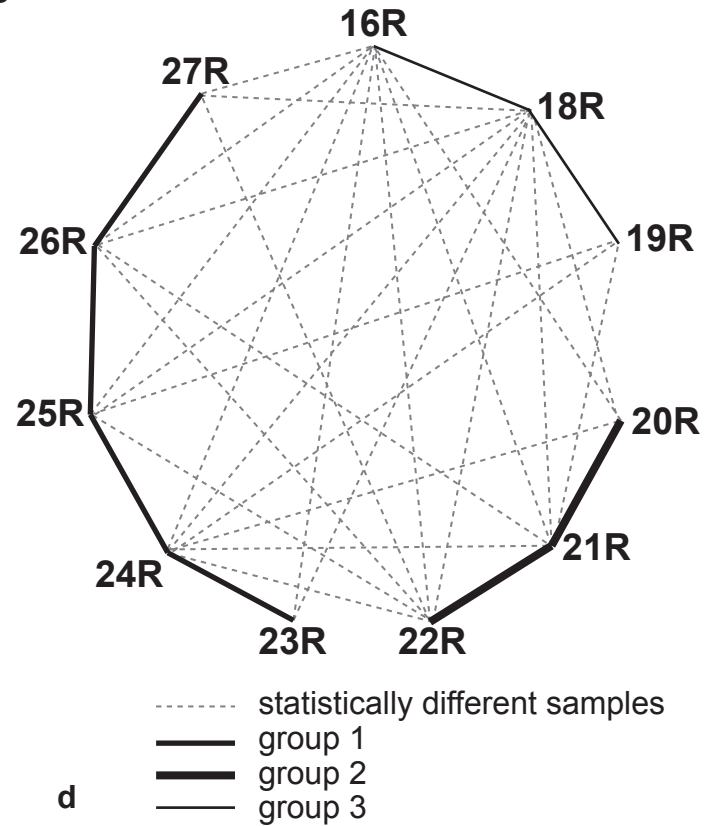
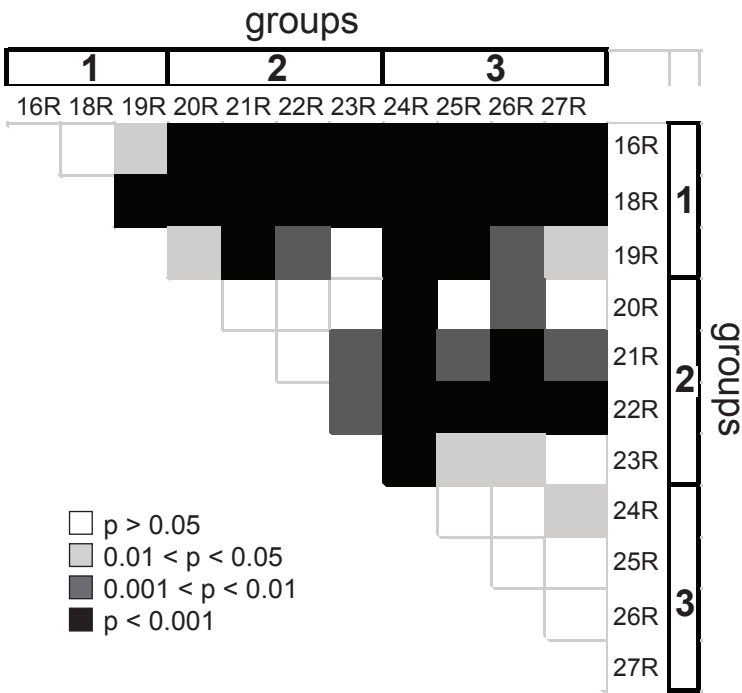
Vergol-La Charce



a

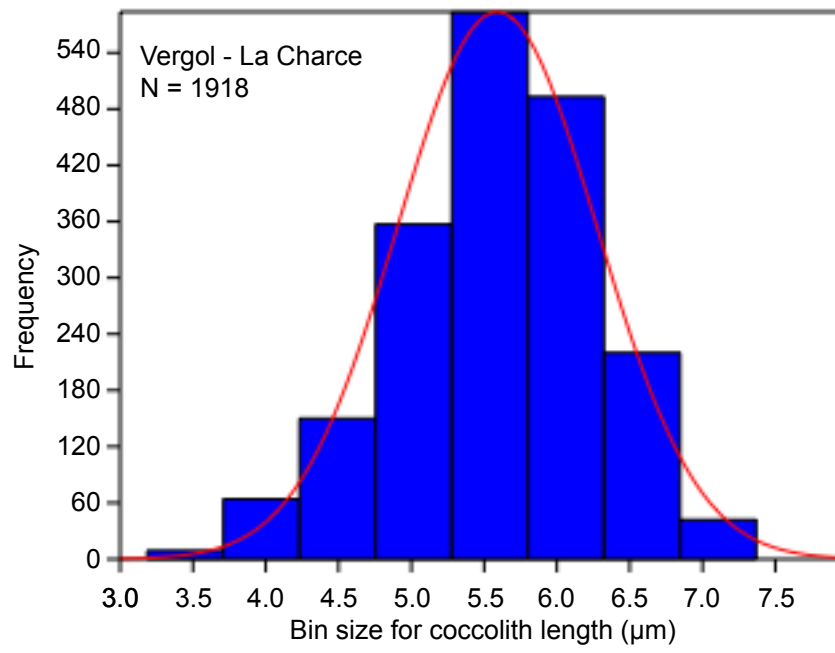
b

ODP Site 1149B

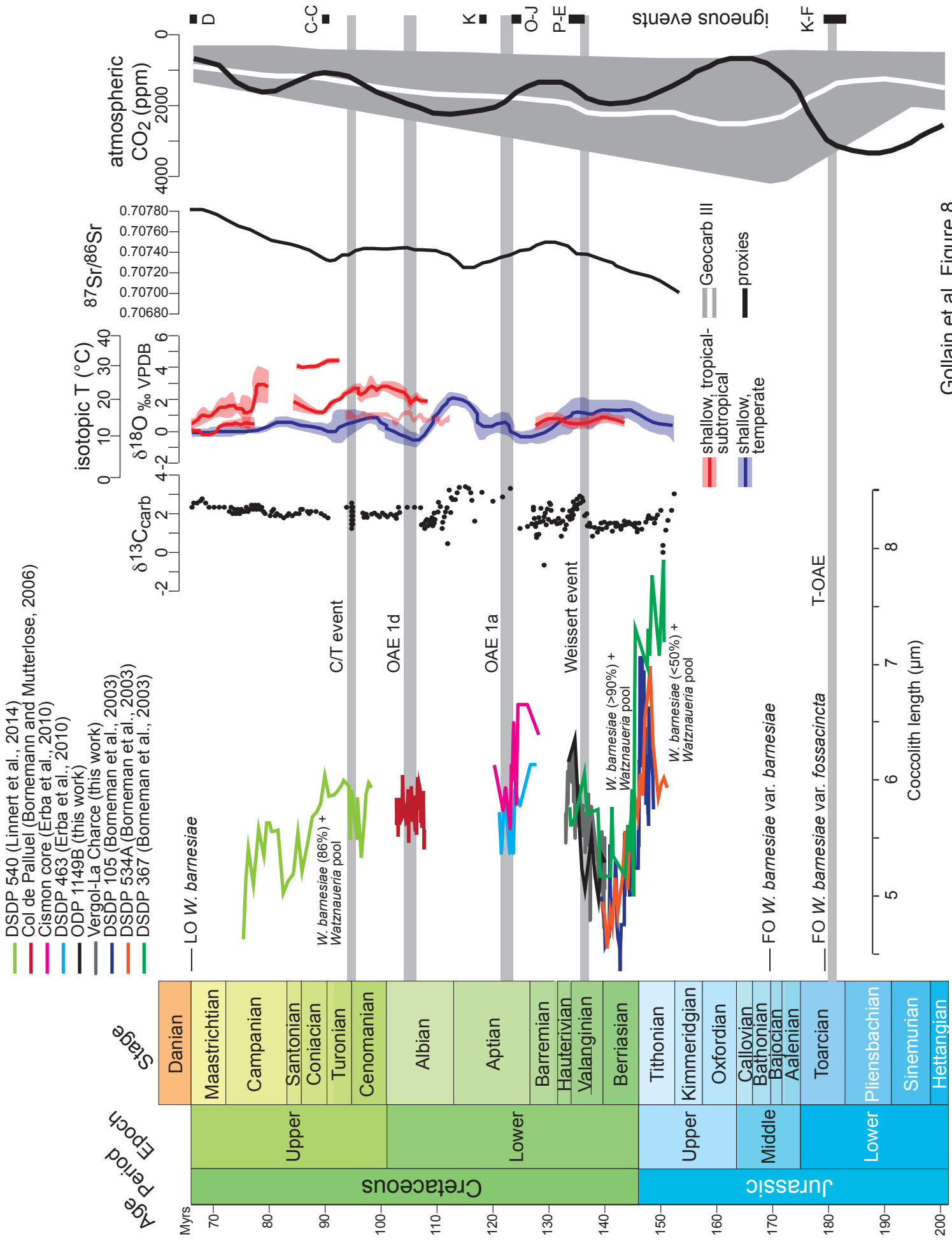


c

d



Gollain et al. Figure 7



Gollain et al. Figure 8